Clinical Radiology 74 (2019) 652.e1–652.e9

Contents lists available at ScienceDirect

Clinical Radiology

journal homepage: www.clinicalradiologyonline.net

Brain SPECT and perfusion MRI: do they provide complementary information about the tumour lesion and its grading?

M. Daboudi [a,*], E. Papadaki [b,c], A. Vakis [d], G. Chlouverakis [e], D. Makrakis [b], D. Karageorgou [b], P. Simos [c,f], S. Koukouraki [a]

[a] Department of Nuclear Medicine, School of Medicine, University of Crete, Heraklion, Crete, Greece
[b] Department of Radiology, School of Medicine, University of Crete, Heraklion, Crete, Greece
[c] Institute of Computer Science, Foundation of Research and Technology, Heraklion, Crete, Greece
[d] Department of Neurosurgery, School of Medicine, University of Crete, Heraklion, Crete, Greece
[e] Biostatistics Lab., Department of Social and Family Medicine, School of Medicine, University of Crete, Heraklion, Crete, Greece
[f] Department of Psychiatry, School of Medicine, University of Crete, Heraklion, Crete, Greece

ARTICLE INFORMATION

Article history:
Received 14 November 2018
Accepted 22 March 2019

AIM: To evaluate the relative and combined utility of ^{99m}Tc-tetrofosmin (^{99m}Tc-TF) brain single-photon-emission computed tomography (SPECT) and dynamic susceptibility contrast (DSC) perfusion magnetic resonance imaging (MRI) in grading brain gliomas.

MATERIALS AND METHODS: Thirty-six patients with clinically suspected brain tumours were assessed by ^{99m}Tc-TF SPECT and DSC-MRI. Brain tumour malignancy was confirmed in all patients at histopathology. On both techniques brain lesions were evaluated via visual and semi-quantitative analysis methods (deriving tetrofosmin index [T-index] and relative cerebral blood volume [rCBV] ratios, respectively).

RESULTS: ^{99m}Tc-TF SPECT showed abnormally elevated tracer uptake in 31/36 patients whereas MRI detected the brain tumour in all patients. Optimal cut-off values of each index for discriminating between low- and high-grade gliomas were obtained through receiver operating characteristic (ROC) analyses. A T-index cut-off of 6.35 ensured 82% sensitivity and 71% specificity for discriminating between high- and low-grade gliomas, whereas a relative rCBV ratio cut-off of 1.80 achieved 91% sensitivity and 100% specificity. Requiring a positive result on either technique to characterise a high-grade glioma was associated with similar specificity and slightly increased sensitivity.

CONCLUSION: Both imaging techniques, ^{99m}TF SPECT and DSC MRI, may provide complementary indices of tumour grade and have an independent diagnostic value for high-risk tumours.

* Guarantor and correspondent: M. Daboudi, Department of Nuclear Medicine, School of Medicine, University of Crete, Heraklion, Crete, 71003, Greece. Tel.: +30 2813408429; fax: +30 281340842.
E-mail address: marlendabou@gmail.com (M. Daboudi).

https://doi.org/10.1016/j.crad.2019.03.025
0009-9260/

Introduction

Malignant brain and central nervous system (CNS) tumours are the third most common cancer in adults and the second most common cancer among children 0–14 years, and the leading cause of cancer-related deaths in this age group, outpacing even leukaemia according to a 2016 report.[1] Gliomas are the most common malignant brain tumours according to the World Health Organization (WHO) with the most aggressive type being glioma grade IV or glioblastoma multiforme (GBM).[2–4]

Accurate diagnosis, staging, and grading (a key determinant of patient survival) are of great clinical importance for patients with GBM. Despite recent advances in imaging technology, accurate definition of brain tumours still requires histopathological assessment, an invasive procedure prone to inherent sampling errors, especially with stereotactic biopsy.[5] A non-negligible rate of non-diagnostic histopathological results (28%) may be obtained due to the regional heterogeneity of gliomas.[6] Therefore, advanced non-invasive diagnostic techniques are very important for optimal evaluation of brain tumours.

Imaging plays an important role providing information about localisation, characterisation of the tumour, and post-treatment surveillance.[7] Magnetic resonance imaging (MRI) is considered as the reference standard imaging procedure for the evaluation of brain tumours. Despite the excellent soft-tissue visualisation of conventional MRI techniques, abnormal contrast enhancement, perilesional oedema, and mass effect, due to non-specific blood–brain barrier (BBB) disruption in both neoplastic and non-neoplastic pathologies, limit the accurate grading of brain tumours.[8–11] More advanced MRI techniques, such as perfusion MRI, have been incorporated into clinical practice to offer better characterisation of brain tumours, providing both structural and functional information at the cellular level. Perfusion MRI can provide crucial information regarding two indices of tumour aggressiveness, tumour neovascularity and capillary permeability, by using the dynamic susceptibility contrast (DSC) and dynamic contrast enhanced (DCE) perfusion techniques, respectively. Tumour neovascularity is reflected in changes in cerebral blood volume (CBV), expressed as rCBV (ratio of tumour CBV to contralateral normal appearing white matter CBV) and has been widely used in clinical practice for the diagnosis, differential diagnosis, surgical planning, and prognosis of brain gliomas.[5,12–29]

Nuclear medicine imaging techniques, namely single-photon-emission computed tomography (SPECT), positron-emission tomography (PET), and hybrid imaging SPECT and PET combined with computed tomography (SPECT/CT, PET/CT), could offer additional information to conventional imaging regarding tumour activity, cell proliferation, and blood flow. Semi-quantitative SPECT analysis showed high uptake of the radiotracer within the tumour compared to the surrounding tissue (retention index) due to the higher metabolic activity of the cells.[30] Several studies showed that higher tracer uptake may be associated with higher-grade gliomas and higher mortality.[31–34] There has been a growing interest in the clinical value of ^{99m}Tc-tetrofosmin (^{99m}Tc-TF) SPECT scintigraphy for identifying and grading brain malignant tumours in the last decades.[35,36] Although ^{99m}Tc-TF does not cross the intact BBB and does not accumulate in normal brain parenchyma, high tracer concentrations are typically achieved within brain tumours via passive transport driven by the negative potential of the intact cell membrane.[37]

Although the utility of ^{99m}Tc-TF SPECT and perfusion MRI techniques has been studied separately, studies comparing the two imaging techniques and assessing their combined value for tumour grading are scarce. The aim of this prospective study is to investigate the potential role of ^{99m}Tc-TF SPECT and perfusion MRI in providing complementary, clinically relevant information regarding tumour grading.

Materials and methods

Over a period of 6 years (2008–2014), 36 patients (20 males, 16 females) with clinically suspected brain tumours were evaluated prospectively. The study was approved by the ethics committee and all patients provided written consent for participating in the study. All patients underwent ^{99m}Tc-TF SPECT of the brain and perfusion MRI on two consecutive days. Surgical excision of the brain lesion or stereotactic biopsy in selected cases was performed within the following week. The final diagnosis was based on excised tissue histology as a reference standard. Informed consent was received from all patients.

Demographic, clinical, and histopathological patient characteristics are shown in Table 1. The sample included 22 patients with high-grade gliomas (15 Grade IV glioblastomas and seven Grade III anaplastic astrocytomas), and 14 patients with low-grade gliomas (Grade II astrocytoma). The two groups had similar proportions of women (45.5% and 42.9%, respectively) and were comparable in average age (62.18±13.7 versus 53.7±19.8 years, respectively, p=0.14).

^{99m}Tc-TF SPECT brain scintigraphy

^{99m}Tc-TF (925 MBq [25mCi]; MyoviewTM, General Electric Healthcare, Buckinghamshire, UK) was given intravenously. Tomographic images were acquired 20–30 minutes after intravenous injection of the radiotracer using a dual-head, tomographic γ-camera (optima NX, GE Medical systems, Waukesha, WI, USA) equipped with a pair of low-energy, high-resolution parallel-hole collimators (LEHR). SPECT images have been reconstructed using filtered back projection with a Butterworth filter. Chang's method was used for attenuation correction.

Qualitative and semi-quantitative analysis was performed independently by two nuclear medicine physicians (M.D., S.K.), using a Xeleris Version 3 Workstation. Qualitative analysis relied on visual analysis of radiotracer accumulation in space-occupying lesions in all three axes (transverse, coronal, and sagittal). Abnormally increased

Table 1
Clinical, imaging, and demographic patient characteristics.

ID	Age	Gender	T-index	rCBV ratio	Diagnosis[a]	Histology/grading
1	51	Male	4.21	2.44	S	Glioma G IV
2	53	Female	6.65	3.59	B	Glioma G III
3	60	Female	8.75	2.59	B	Glioma G IV
4	71	Male	10.9	1.75	S	Glioma G IV
5	77	Female	6.39	1.9	S	Glioma G III
6	57	Male	8.15	2.75	B	Glioma G IV
7	50	Male	11.8	2.88	B	Glioma G III
8	71	Male	10.07	2.95	B	Glioma G IV
9	76	Male	7.16	2.64	S	Glioma G IV
10	26	Female	10.7	1.87	S	Glioma G III
11	64	Female	10.28	2.71	B	Glioma G IV
12	40	Male	—[b]	1.61	B	Glioma G III
13	57	Male	8.17	3.3	B	Glioma G III
14	57	Female	4.75	2.18	B	Glioma G IV
15	63	Female	7.48	1.5	B	Glioma G IV
16	55	Male	4.12	1.78	B	Glioma G III
17	67	Male	8.28	1.78	S	Glioma G IV
18	73	Female	6.05	2.94	S	Glioma G IV
19	86	Male	9.6	1.76	S	Glioma G IV
20	72	Female	7	2.92	B	Glioma G IV
21	63	Female	7.48	1.99	S	Glioma G IV
22	79	Female	9.97	2.28	S	Glioma G IV
23	27	Male	—[b]	1.03	S	Glioma G II
24	25	Female	—[b]	0.95	S	Glioma G II
25	66	Female	6.2	1.52	B	Glioma G II
26	65	Female	3.45	1.22	B	Glioma G II
27	70	Male	4.65	1.68	B	Glioma G II
28	59	Male	4.06	1.2	S	Glioma G II
29	80	Male	2.8	1.61	B	Glioma G II
30	67	Male	—[b]	1.15	B	Glioma G II
31	52	Male	2.72	1.21	B	Glioma G II
32	61	Male	6.09	1.26	B	Glioma G II
33	53	Female	3.45	0.87	S	Glioma G II
34	75	Female	3	1.41	B	Glioma G II
35	23	Female	—[b]	1.12	S	Glioma G II
36	29	Female	2.85	1.56	B	Glioma G II

G, grade.
[a] Tumour grade based on histopathology of surgical sample (S) or sample acquired through stereotactic biopsy (B).
[b] Tracer undetectable.

radiotracer uptake over the affected region within the brain parenchyma compared to background was considered indicative of tumour. Semi-quantitative analysis employed circular regions of interest (ROIs) drawn manually on the section traversing the area with the highest mean tracer uptake. An identical ROI was drawn symmetrically (mirror) on the contralateral side of the normal brain parenchyma in the same section. TF index (T-index) values were calculated by dividing the average counts in the tumour region (T) by those in the contralateral normal region (N) for each patient. Inter-rater reliability of measurements (T-index values) performed by two nuclear medicine physicians (M.D. and S.K.) was excellent (intraclass correlation coefficient=0.93).

MRI technique

All patients underwent brain MRI using a 1.5 T whole-body MRI system (Vision/Sonata, Siemens, Erlangen, Germany), equipped with high-performance gradients (gradient strength: 40 mT/m, slew rate: 200 mT/m/ms) and a standard two-channel circularly polarised head-array coil. The protocol for brain tumours comprised the following sequences: (1) three dimensional (3D) T1-weighted (W) ultrafast gradient echo (3D MPRAGE: TR=1,570 ms, TE=1.73 ms, 1 mm^3, number of excitations (NEX)=1/160 axial slices), (2) T2W turbo spin echo (TSE: TR=5,000 ms, TE=98 ms) with 4-mm axial sections, and (3) TSE fluid-attenuated inversion recovery (FLAIR) (TR=9,000 ms, TE=120 ms, TI=2,600 ms) with 4-mm axial and sagittal sections.

The T2* DSC-MRI was performed utilising a two-dimensional (2D) single-shot multisection gradient echo (GRE) echo planar imaging (EPI) sequence (TR=1,500 ms, TE=40 ms, flip angle=30°, bandwidth=2,442 Hz/pixel, echo spacing=0.47 ms, EPI factor=64). A square field of view (FOV) of 192×192 mm^2 and a reconstruction matrix of 64×64 pixels were used. Twenty consecutive sections of 4 mm section thickness with a 1.5 mm intersection gap were obtained in an oblique axial plane covering the whole brain.

The sequence was repeated every 1.5 seconds for a total time of 1 minute 20 seconds, thus obtaining 50 dynamic acquisitions (images) with 1.5 seconds temporal resolution for each of the 20 anatomical sections. Immediately after the end of the fifth dynamic acquisition, a bolus of 0.1 mmol/kg body weight of gadobutrol (Gadovist, Bayer, Leverkusen, Germany) was injected through a catheter inserted in the antecubital vein, at an injection rate of 4 ml/s, immediately followed by a bolus injection of 15 ml saline at the same rate. Contrast-enhanced 3D T1W images were obtained after the acquisition of the perfusion data.

Post-processing of the perfusion data was performed utilising standard software provided by the manufacturer. The DSC-MRI perfusion technique was based on a standard tracer kinetic model with arterial input function (AIF) calculation and a deconvolution method based on a singular value decomposition (SVD) algorithm. The AIF was calculated by manually defining a major artery (usually the major cerebral artery [MCA]) and parametric maps of cerebral blood volume (CBV) were automatically created. CBV values were measured in ROIs located at the tumoural areas with the highest vascularity and the contralateral normal-appearing white matter (NAWM). In order to optimise reproducibility, three CBV measurements were obtained from each of tumoural and NAWM and areas, which were then averaged. All ROIs were fixed in size (radius of 2 mm) and were placed at the bolus peak of the GRE-EPI images, which show the vessels to better advantage and thus vascular structures were excluded. T2W images were also used for co-registration with the GRE-EPI images to ensure that white matter lesions were not included in the ROI. From the GRE-EPI images, ROIs were automatically transferred to the CBV maps using dedicated software (MRIcro medical analysis viewer). ROIs were placed at the same cross-sectional positions and the same locations with those of ^{99m}TcTF SPECT, as described previously.

Perfusion measurements were carried out by three experienced investigators (E.P., D.K., and D.M.) who developed common criteria and procedures to ensure proper placement of multiple ROIs. CBV measurements were conducted independently by each investigator with excellent

inter-rater reliability among them with respect to estimating individual CBV ratios (intraclass correlation coefficient=0.95).

Statistical analysis

T-index and rCBV ratio values did not vary significantly with gender or age (within tumour grade groups; $p>0.3$). Normality of the T-index and rCBV ratio values was assessed using the Shapiro–Wilk test. Tumour grade group differences on each measure were evaluated with one-way analysis of variance (ANOVA; effect size for the group difference were also computed using Cohen's d). Pearson correlation coefficients were used to examine the relation between T-index and rCBV ratio values, both across and within tumour grade groups. Finally, receiver operating characteristic (ROC) curve analyses were employed to identify cut-off values for each index for optimal discrimination between tumour grade groups. Due to the high clinical cost of missing a high-grade tumour, inconclusive SPECT results were treated as positive results to compute the final diagnostic value indices for each test presented in Table 3.[38] All statistical analyses were carried out at the two-sided 5% level of significance using SPSS (Armonk, NY: IBM Corp, USA).

Results

Based on qualitative analysis, SPECT imaging showed variable tracer uptake ranging from faint to intense uptake. ^{99m}Tc-TF SPECT showed abnormally intense uptake in 31/36 patients with low- and high-grade gliomas (detection rate 86.1%; Figs 1–4). False-negative results were observed in 4/14 low-grade tumour cases (28.5%) and in 1/22 high-grade tumour cases (4.5%) resulting in an overall clinical yield of 86% (Figs 5 and 6). rCBV ratio and T-index value distributions did not significantly deviate from normality (Shapiro–Wilk test: $p>0.1$) and, as expected, varied significantly as a function of tumour grade. The T-index ranged between 2.7 and 6.2 in low-grade gliomas ($n=14$) and between 4.12 and 11.8 in high-grade gliomas ($F(1,29)=28.87$, $p<0.001$, Cohen's d=1.48; Fig 7). Corresponding values for rCBV were 0.87–1.68 and 1.5 to 3.59, respectively ($F(1,34)=42.62$, $p<0.001$, Cohen's d=1.49).

Table 2
Frequency of positive, negative, and inconclusive SPECT and rCBV results against histopathological diagnosis.

	Biopsy					
	Low			High		
	Low (TN)	High (FP)	Inconclusive	Low (FN)	High (TP)	Inconclusive
rCBV	14	0	0	2	20	0
SPECT	10	0	4	4	17	1
rCBV or SPECT	14	0	-	1	21	-
rCBV and SPECT	10	0	4	5	16	1

rCBV, relative cerebral blood volume; SPECT, single-photon-emission computed tomography; TN, true negative; FN, false negative; FP, false positive; TP, true positive.

Table 3
Diagnostic accuracy indices for SPECT and rCBV.

	Sensitivity (%)	Specificity (%)	PPV (%)	NPV (%)
rCBV	91	100	100	88
SPECT	82	71	82	71
rCBV or SPECT	95	100	100	93
rCBV and SPECT	76	100	100	67

Computed in the entire sample. Cut-off values; T-index=6.35, rCBV ratio=1.80.
rCBV, relative cerebral blood volume; SPECT, single-photon-emission computed tomography; PPV, positive predictive value; NPV, negative predictive value.

Direct comparisons between rCBV ratios and T-index values were restricted to cases where valid SPECT data were obtained ($n=31$). Across tumour groups there was a modest linear association between the two measures ($r=0.51$, $p<0.003$), but closer inspection revealed that this association was largely due to group differences in both measures (Fig 8). Within each group, the correlation between the two measures did not reach significance ($r<0.1$).

ROC analyses were conducted in order to derive optimal cut-off values for rCBV ratio ($n=36$) and T-index values ($n=31$ excluding inconclusive tests) in discriminating between patient groups (Fig 9). To ensure fair comparison between the two methods, however, accuracy indices were estimated on the entire sample ($n=36$). Due to the high clinical cost of missing a high-grade tumour, inconclusive SPECT results were treated as positive results to compute the final diagnostic value indices for each test. Results indicated that a T-index cut-off value of 6.35 ensured 82% sensitivity and 71% specificity in discriminating between low- and high-grade gliomas, whereas a cut-off rCBV ratio of 1.80 achieved 91% sensitivity and 100% specificity (Tables 2 and 3). Combining data from the two methods, so that a positive (high grade) outcome required the above cut-off values on either test, resulted in a slight improvement in sensitivity (95%) without reduction in specificity (100%).

Discussion

Gliomas are the most common primary neoplasms of the brain, varying from low to high grade, with GBM having the poorest prognosis. Discrimination between low- and high-grade gliomas before surgical intervention is critical for clinical management. In recent years, more advanced MRI and nuclear medicine techniques have been employed to differentiate malignant and non-neoplastic brain lesions and contribute to the preoperative characterisation of tumour grading.[39–41] Perfusion MRI measures CBV inside the lesion relative to the contralateral healthy tissue (rCBV). Increased rCBV reflects the degree of tumour neovascularity—a pathophysiological process that is considered an index of tumour aggressiveness.[29] Nuclear medicine techniques, i.e., PET, SPECT, and hybrid imaging techniques PET/CT, SPECT/CT, have also been used for the evaluation of

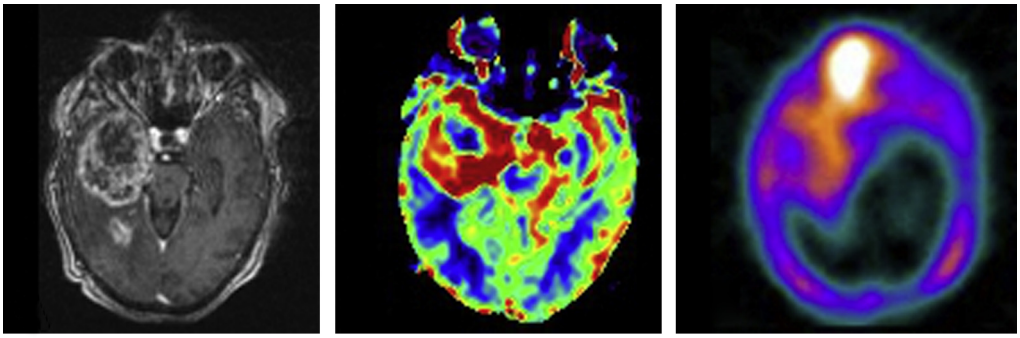

Figure 1 Imaging data from a 63-year-old woman with glioblastoma. (a) Post-gadolinium T1W MPRAGE sequence demonstrates an inhomogeneously enhancing space-occupying lesion in the right temporal lobe, with enhancing solid tissue and central necrotic areas. (b) Relative CBV values are high in the solid tumoural tissue (red on the rCBV map) averaging 1.99 due to increased vascularity. (c) ^{99m}Tc-TF SPECT shows highly increased uptake in the right temporal region with a T-index of 7.48.

brain lesions. Recently, ^{99m}Tc-labelled compounds, ^{99m}Tc methoxyisobutylisonitrile (MIBI) and ^{99m}Tc-TF, are found to be advantageous as compared to Thalium-201 due to lower radiation exposure to patients and improved spatial resolution.[36] ^{99m}Tc-TF, a marker of regional blood flow and cell membrane activity, is a lipophilic tracer with no uptake in normal brain due to its mechanism of uptake based on the intact BBB.

In the present prospective study, the potential contribution of TF in differentiating tumours with different biological behaviour, namely low- and high-grade gliomas, was explored. Specifically, the clinical yield and accuracy of DSC MRI and ^{99m}Tc-TF SPECT were compared in differentiating low-from high-grade gliomas against histopathological diagnosis as the standard diagnostic tool. In the present study ^{99m}Tc-TF SPECT had a lower detection rate compared to MRI (86% versus 100%). The reason for the inability to detect all 36 tumour lesions is not entirely clear. Possible explanations causing inadequate TF uptake include tumour location and size, atypically low tumour blood supply, maintenance of cell membrane integrity, and failure of the tumour to disrupt the BBB.[35] These effects are more likely to occur in the presence of low-grade tumours as in the majority of inconclusive SPECT studies in the present patient series. False-negative results were obtained in four patients with low-grade tumours and in one patient with anaplastic glioma. In one patient with low-grade glioma, there was a small lesion (<1 cm), which is below the spatial resolution of the γ camera); two patients with low-grade glioma had lesions without gadolinium enhancement on MRI (suggesting lack of disruption of the BBB). Finally, two patients presented tumours (a low-grade glioma and an anaplastic glioma) with extensive perilesional oedema on conventional MRI that can affect tracer uptake. Petrovic *et al.* using radionuclide angiography documented extensive perfusion variability both across and within tumour grades, showing that perfusion of low-grade gliomas was similar to that of contralateral normal brain, in contrast to the perfusion of high-grade tumours that was higher.[42]

Regarding the capacity of perfusion MRI to discriminate between high- and low-grade tumours, the present results compare favourably with previous reports. In the present study, rCBV ratio values ranged between 0.87 and 1.68 for low-grade tumours and between 1.5 and 3.59 for high-grade tumours. Based on ROC analyses, an optimised cut-off value of 1.80 yielded sensitivity and specificity of 91%

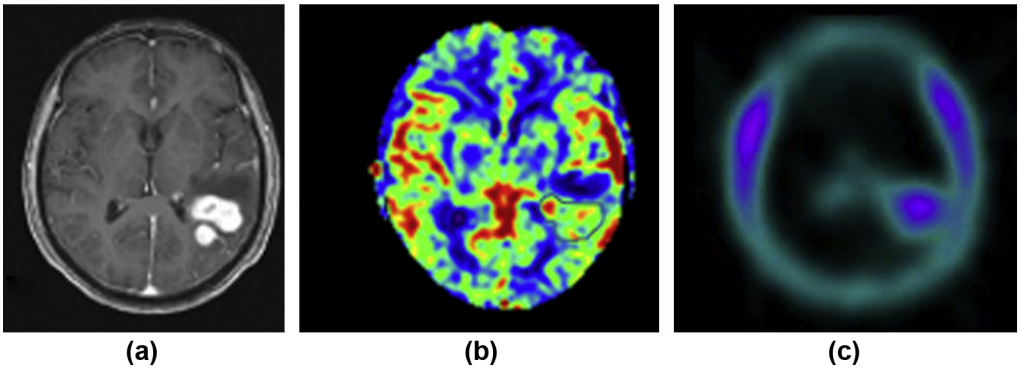

Figure 2 Imaging data from a 66-year-old woman with a low-grade astrocytoma. (a) Post-gadolinium T1W MPRAGE sequence reveals a lobulate, enhancing lesion in the left parietal lobe that compresses the trigone of the left lateral ventricle. (b) The average relative CBV value of the lesion (blue shape on the rCBV map) is 1.52. (c) ^{99m}Tc-TF SPECT reveals increased uptake in the left occipitoparietal region, with a T-index of 6.2.

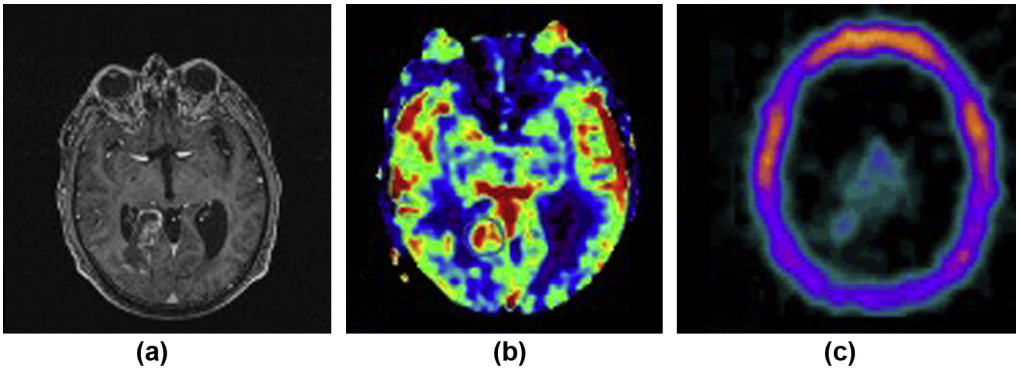

Figure 3 Imaging data from a 70-year-old man with a low-grade astrocytoma. (a) Post-gadolinium T1W MPRAGE sequence reveals a space-occupying lesion in the right occipital lobe, with a central cystic portion and peripheral enhancement compressing the right occipital horn. (b) The average relative CBV value of the enhancing portion of the lesion (blue shape on the rCBV map) is 1.68. (c) ^{99m}Tc-TF SPECT reveals increased uptake in the right occipital lobe with a T-index 4.65.

and 100%, respectively, for distinguishing high-from low-grade tumours. Several studies report the utility of perfusion MRI and the value of the rCBV ratio in distinguishing low-from high-grade brain tumours. In the earliest studies, a rCBV cut-off of 1.75 was found to afford 95% sensitivity and 57% specificity in differentiating low-from high-grade gliomas[21,22]; however, other studies cast doubt on the utility of this technique, reporting highly variable sensitivity

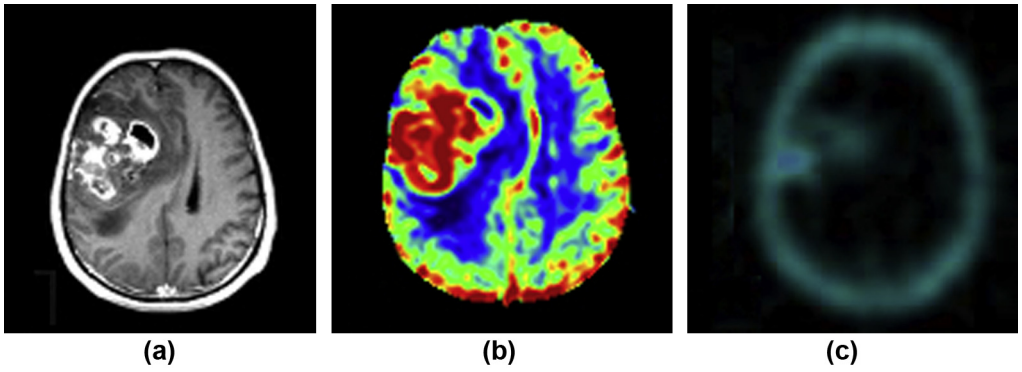

Figure 4 Imaging data from a 57-year-old woman with glioblastoma. (a) Post-gadolinium T1W MPRAGE sequence demonstrates a large, lobular, inhomogeneously enhancing space-occupying lesion in the right frontal lobe, with enhancing solid tissue and small necrotic areas, surrounded by extensive perilesional oedema, and deviation of middle-line structures to the left. (b) Relative CBV values are very high in the solid tumoural tissue (red on the rCBV map) averaging 3.3 due to highly increased vascularity. (c) ^{99m}Tc-TF SPECT shows increased uptake in the right frontal lobe with a T-index 8.17.

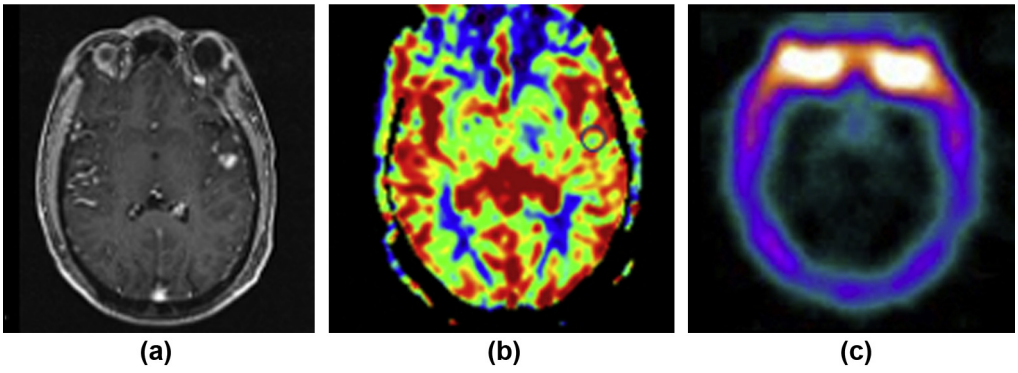

Figure 5 Imaging data from a 27-year-old man with a low-grade astrocytoma. (a) Post-gadolinium T1W MPRAGE sequence demonstrates a small, enhancing nodule located in the upper left temporal lobe. (b) The average relative CBV value of the lesion (blue shape on the rCBV map) is 1.03, indicative of low vascularity. (c) ^{99m}Tc-TF SPECT showed normal uptake in the brain parenchyma, possibly due to the small size of the lesion ($<$1 cm).

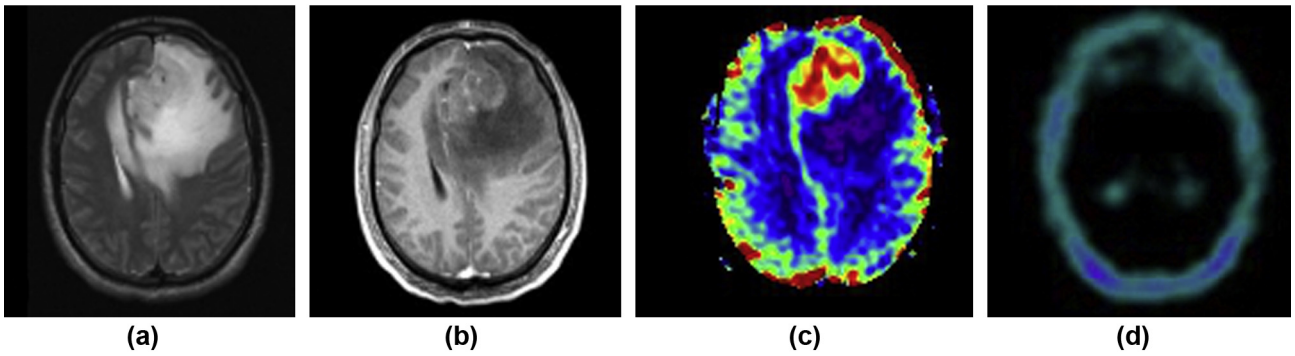

Figure 6 Imaging data from a 40-year-old man with an anaplastic astrocytoma. (a) T2W TSE sequence reveals a space-occupying tumour in the left frontal lobe, surrounded by extensive perilesional oedema, with deviation of middle-line structures to the right. (b) The lesion is characterised by inhomogeneous enhancement on the post-gadolinium T1W MPRAGE sequence. (c) The tumour is apparent on the perfusion map with an average relative CBV value of 1.61. (d) ^{99m}Tc-TF SPECT did not show pathological uptake possibly due to extensive oedema.

(ranging from 66% to 93%) and specificity (ranging from 9% to 90%).[12–14,42,43] According to a recent review summarising results from 115 participants selected from published and unpublished data sets, the average rCBV of 83 low-grade and 32 high-grade gliomas were 1.29 (95% CI: 0.01 to 5.10) and 1.89 (95% CI: 0.30 to 6.51), respectively, with an aggregate sensitivity of 83% and specificity of 48% (using the rCBV cut-off of 1.75).[12] The authors concluded that a larger number of both high- and low-grade gliomas, use of a standardised scanning approach, and an updated reference standard incorporating molecular profiles, are required to draw firm conclusions.

Adopting an optimised cut-off T-index value of 6.35, the sensitivity of SPECT in the current study was comparable to that obtained using perfusion MRI (82 versus 91%); however, the specificity of the former method was considerably lower (71 versus 100%), mainly due to the treatment of inconclusive SPECT results as positive results in the analyses. Few studies have evaluated the potential contribution of ^{99m}Tc-TF SPECT imaging in distinguishing low-from high-grade tumours.[8,35,36] In the largest reported consecutive patient series (n=106),[8] TF uptake was significantly increased in high-grade gliomas (n=45; T-index=8.25±5.6) versus low-grade gliomas (n=6; T-index=3.16±2.26). Using ROC analysis, the optimal cut-off value of 2.8 achieved 91.3% sensitivity and 83.3% specificity in distinguishing between the two groups. Only one study has directly compared ^{99m}Tc-TF SPECT with perfusion MRI results. On a consecutive series of 25 operated tumour patients, Alexiou *et al.*[44] reported perfect sensitivity and specificity in distinguishing 21 high-grade from only four low-grade gliomas (n=4; using a T-index cut-off of 2.8). Corresponding values for an rCBV ratio cut-off of 0.63 were 100% sensitivity and 94.4% specificity. In the present patient series, a considerably

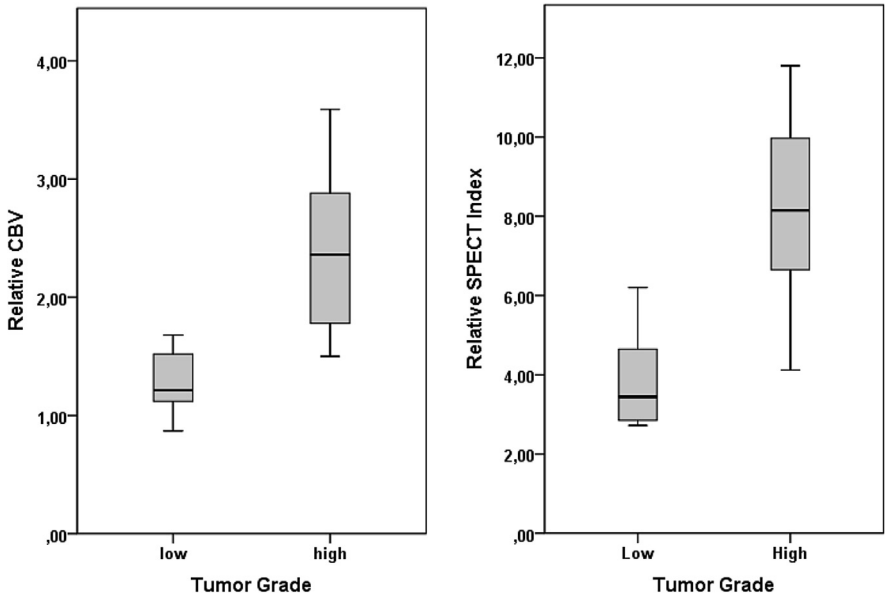

Figure 7 Box-plots of SPECT values (T-index; right-hand panel) and relative CBV values (left-hand panel) by tumour grade group. Boxes indicate interquartile range of values. Overall, tumour group differences were similar across indices as reflected in effect sizes (Cohen's d=1.48 and 1.49, respectively).

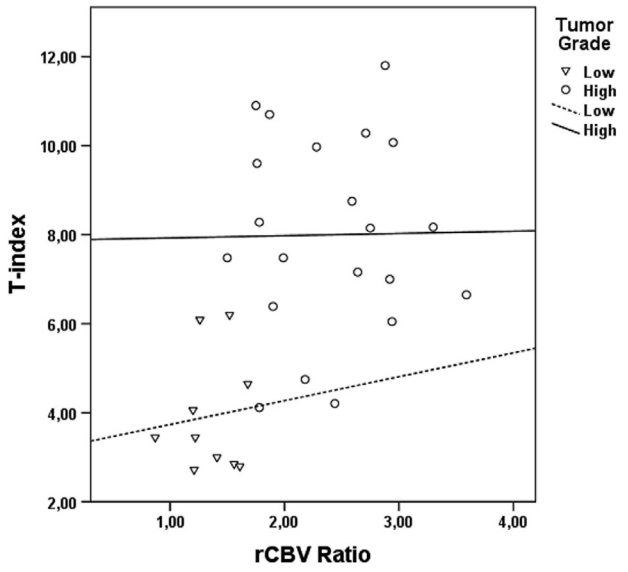

Figure 8 Scatterplot illustrating the association between SPECT measurements (T-index) and rCBV ratio values among patients with low-grade (triangles/dashed regression line) and patients with high-grade tumours (circles/solid regression line). R^2=0.26 across groups (n=31).

higher T-index cut-off was associated with optimal, yet moderately successful, discrimination of histopathology-based tumour grade. This apparent discrepancy may be attributed to two main features of the data: (1) inconclusive SPECT results were included in the analyses comparing the two techniques by adopting a clinically oriented conservative approach of considering them as positive (i.e., potentially indicative of a high grade tumour); and (2) three patients with high-grade gliomas on histopathology biopsy were included in the analysis who displayed unusually low TF uptake within the tumour tissue, probably due the scarcity of viable cells inside the tumour.

The main limitations of the present study are the relatively small number of patients and the unavailability of SPECT/CT. Further studies with larger sample sizes are required to reach firm conclusions regarding the optimal preoperative approach to characterise brain malignancies. Importantly, the validity of the cut-off values established and tested in the current study for each imaging method requires independent validation on a different sample of patients comprising comparable numbers of tumour grades.

In conclusion, employing ^{99m}Tc-TF SPECT and perfusion MRI as complementary indices of tumour grade (i.e., by relying on positive findings of either technique for diagnosis) ensures the same specificity and positive predictive value in comparison with perfusion MRI alone and slightly *increased* sensitivity and negative predictive value; however, requiring converging classification of tumour grade by both techniques was associated with significantly reduced sensitivity and negative predictive value than perfusion MRI. Both SPECT and perfusion MRI, may convey significant clinical information regarding tumour grading and have an independent diagnostic value for high-risk tumours.

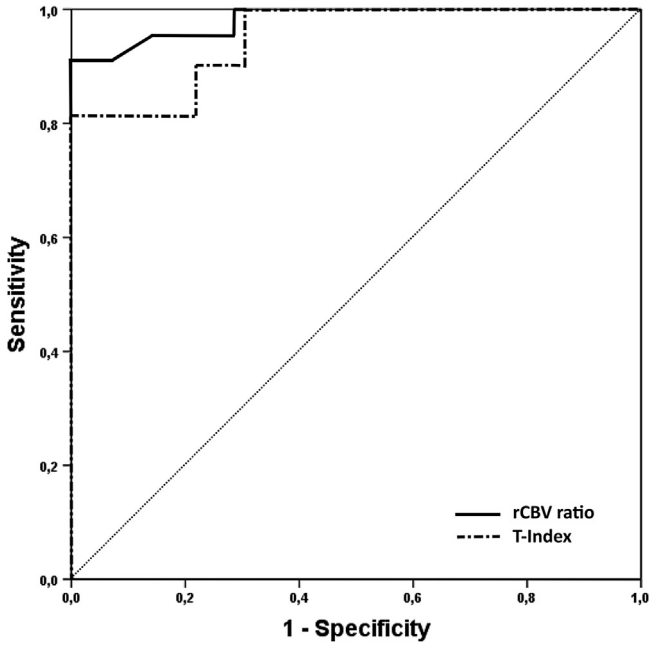

Figure 9 Comparison of ROC curves in discriminating between high- and low-grade gliomas based on either relative rCBV ratios (area under the curve [AUC]=0.982, SE=0.017, p<0.001) or T-index values (AUC=0.952, SE=0.035, p<0.001).

Conflict of interest

The authors declare no conflict of interest.

References

1. American Brain Tumour Association. Brain tumor education. Available at: https://www.abta.org/about-brain-tumors/brain-tumor-education/ [Accessed 25/01/2017].
2. Alifieris C, Trafalis DT. Glioblastoma multiforme: pathogenesis and treatment. *Pharmacol Ther* 2015;**152**:68–83. https://doi.org/10.1016/j.pharmthera.2015.05.005.
3. Thakkar JP, Dolecek TA, Horbinski C, *et al*. Epidemiologic and molecular prognostic review of glioblastoma. *Cancer Epidemiol Biomarkers Prev* 2014;**23**(10):1985–96. https://doi.org/10.1158/1055-9965.EPI-14-0275.
4. Holland EC. Glioblastoma multiforme: the terminator. *Proc Natl Acad Sci* 2000;**97**(12):6242–4. https://doi.org/10.1073/pnas.97.12.6242.
5. Santarosa C, Castellano A, Conte GM, *et al*. Dynamic contrast-enhanced and dynamic susceptibility contrast perfusion MR imaging for glioma grading: preliminary comparison of vessel compartment and permeability parameters using hotspot and histogram analysis. *Eur J Radiol* 2016;**85**(6):1147–56. https://doi.org/10.1016/j.ejrad.2016.03.020.
6. Park KJ, Kang SH, Park DH, *et al*. Usefulness of thallium-201 SPECT for prediction of early progression in low-grade astrocytomas diagnosed by stereotactic biopsy. *Clin Neurol Neurosurg* 2012;**114**(3):223–9. https://doi.org/10.1016/j.clineuro.2011.10.023.
7. Treister D, Kingston S, Hoque KE, *et al*. Multimodal magnetic resonance imaging evaluation of primary brain tumours. *Semin Oncol* 2014;**41**(4):478–95. https://doi.org/10.1053/j.seminoncol.2014.06.006.
8. Fotopoulos AD, Kyritsis AP, Tsiouris S, *et al*. Characterization of intracranial space-occupying lesions by ^{99m}Tc-tetrofosmin SPECT. *J Neurooncol* 2011;**101**(1):83–9. https://doi.org/10.1007/s11060-010-0230-9.
9. Al-Okaili RN, Krejza J, Woo JH, *et al*. Intraaxial brain masses: MR imaging–based diagnostic strategy—initial experience. *Radiology* 2007;**243**(2):539–50.

10. Runge VM, Muroff LR, Jinkins JR. Central nervous system: review of clinical use of contrast media. *Top Magn Reson Imaging* 2001;**12**(4):231–63.
11. Watanabe M, Tanaka R, Takeda N. Magnetic resonance imaging and histopathology of cerebral gliomas. *Neuroradiology* 1992;**32**:463–9.
12. Abrigo JM, Fountain DM, Provenzale JM, *et al.* Magnetic resonance perfusion for differentiating low-grade from high-grade gliomas at first presentation. *Cochrane Database Syst Rev* 2018;**1**:CD011551. https://doi.org/10.1002/14651858.CD011551.pub2.
13. Boxerman JL, Shiroishi MS, Ellingson BM, *et al.* Dynamic susceptibility contrast MR imaging in glioma. *Magn Reson Imaging Clin N Am* 2016;**24**(4):649–70. https://doi.org/10.1016/j.mric.2016.06.005.
14. Arevalo-Perez J, Peck KK, Young RJ, *et al.* Dynamic contrast-enhanced perfusion MRI and diffusion-weighted imaging in grading of gliomas. *J Neuroimaging* 2015;**25**(5):792–8. https://doi.org/10.1111/jon.12239.
15. Zhang J, Liu H, Tong H, *et al.* Clinical applications of contrast-enhanced perfusion MRI techniques in gliomas: recent advances and current challenges. *Contrast Media Mol Imaging* 2017;**2017**:1–27. https://doi.org/10.1155/2017/7064120.
16. Jain R, Gutierrez J, Narang J, *et al.* In vivo correlation of tumour blood volume and permeability with histologic and molecular angiogenic markers in gliomas. *Am J Neuroradiol* 2011;**32**(2):388–94. https://doi.org/10.3174/ajnr.A2280.
17. Barajas RF, Cha S. Benefits of dynamic susceptibility-weighted contrast-enhanced perfusion MRI for glioma diagnosis and therapy. *CNS Oncol* 2014;**3**(6):407–19. https://doi.org/10.2217/cns.14.44.
18. Hylton N. Dynamic contrast-enhanced magnetic resonance imaging as an imaging biomarker. *J Clin Oncol* 2006;**24**(20):3293–8. https://doi.org/10.1200/JCO.2006.06.8080.
19. Shiroishi MS, Castellazzi G, Boxerman JL, *et al.* Principles of T_2^*-weighted dynamic susceptibility contrast MRI technique in brain tumour imaging. *J Magn Reson Imaging* 2015;**41**(2):296–313. https://doi.org/10.1002/jmri.24648.
20. Maia ACM, Malheiros SMF, da Rocha AJ, *et al.* MR cerebral blood volume maps correlated with vascular endothelial growth factor expression and tumour grade in nonenhancing gliomas. *AJNR Am J Neuroradiol* 2005;**26**(4):777–83.
21. Law M, Yang S, Wang H, *et al.* Glioma grading: sensitivity, specificity, and predictive values of perfusion MR imaging and proton MR spectroscopic imaging compared with conventional MR imaging. *AJNR Am J Neuroradiol* 2003;**24**(10):1989–98.
22. Law M, Yang S, Babb JS, *et al.* Comparison of cerebral blood volume and vascular permeability from dynamic susceptibility contrast-enhanced perfusion MR imaging with glioma grade. *AJNR Am J Neuroradiol* 2004;**25**(5):746–55.
23. Server A, Graff BA, Orheim TED, *et al.* Measurements of diagnostic examination performance and correlation analysis using microvascular leakage, cerebral blood volume, and blood flow derived from 3T dynamic susceptibility-weighted contrast-enhanced perfusion MR imaging in glial tumour grading. *Neuroradiology* 2011;**53**(6):435–47. https://doi.org/10.1007/s00234-010-0770-x.
24. Aprile I, Giovannelli G, Fiaschini P, *et al.* High- and low-grade glioma differentiation: the role of percentage signal recovery evaluation in MR dynamic susceptibility contrast imaging. *Radiol Med* 2015;**120**:967–74. https://doi.org/10.1007/s11547-015-0511-7.
25. Falk A, Fahlström M, Rostrup E, *et al.* Discrimination between glioma grades II and III in suspected low-grade gliomas using dynamic contrast-enhanced and dynamic susceptibility contrast perfusion MR imaging: a histogram analysis approach. *Neuroradiology* 2014;**56**(12):1031–8. https://doi.org/10.1007/s00234-014-1426-z.
26. Liu X, Tian W, Kolar B, *et al.* MR diffusion tensor and perfusion-weighted imaging in preoperative grading of supratentorial nonenhancing gliomas. *Neuro Oncol* 2011;**13**(4):447–55. https://doi.org/10.1093/neuonc/noq197.
27. Morita N, Wang S, Chawla S, *et al.* Dynamic susceptibility contrast perfusion weighted imaging in grading of nonenhancing astrocytomas. *J Magn Reson Imaging* 2010;**32**(4):803–8. https://doi.org/10.1002/jmri.22324.
28. Sahin N, Melhem ER, Wang S, *et al.* Advanced MR imaging techniques in the evaluation of nonenhancing gliomas: perfusion-weighted imaging compared with proton magnetic resonance spectroscopy and tumour grade. *Neuroradiol J* 2013;**26**(5):531–41. https://doi.org/10.1177/197140091302600506.
29. Hardee ME, Zagzag D. Mechanisms of glioma-associated neovascularization. *Am J Pathol* 2012;**181**(4):1126–41. https://doi.org/10.1016/j.ajpath.2012.06.030.
30. Henkin R. *Nuclear medicine*. St Louis, MI: Mosby; 2006. p. 1–7.
31. Schwartz RB, Holman BL, Polak JF, *et al.* Dual-isotope single-photon emission computerized tomography scanning in patients with glioblastoma multiforme: association with patient survival and histopathological characteristics of tumour after high-dose radiotherapy. *J Neurosurg* 1998;**89**(1):60–8. https://doi.org/10.3171/jns.1998.89.1.0060.
32. Alexiou GA, Tsiouris S, Kyritsis AP, *et al.* The value of ^{99m}Tc-tetrofosmin brain SPECT in predicting survival in patients with glioblastoma multiforme. *J Nucl Med* 2010;**51**(12):1923–6. https://doi.org/10.2967/jnumed.110.080929.
33. Prigent-Le Jeune F, Perez S, Dubois F, *et al.* Technetium-^{99m} sestamibi brain SPECT in the follow-up of glioma for evaluation of response to chemotherapy: first results. *Eur J Nucl Med Mol Imaging* 2004;**31**(5):714–9. https://doi.org/10.1007/s00259-004-1463-7.
34. Kallén K, Burtscher IM, Holtås S, *et al.* ^{201}Thallium SPECT and ^{1}H-MRS compared with MRI in chemotherapy monitoring of high-grade malignant astrocytomas. *J Neurooncol* 2000;**46**(2):173–85.
35. Soricelli A, Cuocolo A, Varrone A, *et al.* Technetium-99m-tetrofosmin uptake in brain tumours by SPECT: comparison with thallium-201 imaging. *J Nucl Med* 1998;**39**(5):802–6.
36. Choi JY, Kim SE, Shin HJ, *et al.* Brain tumour imaging with ^{99m}Tc-tetrofosmin: comparison with 201Tl, ^{99m}Tc-MIBI, and ^{18}F-fluorodeoxyglucose. *J Neurooncol* 2000;**46**(1):63–70.
37. Fotopoulos AD, Alexiou GA, Goussia A, *et al.* ^{99m}Tc-Tetrofosmin brain SPECT in the assessment of meningiomas—correlation with histological grade and proliferation index. *J Neurooncol* 2008;**89**(2):225–30. https://doi.org/10.1007/s11060-008-9611-8.
38. Shinkins B, Thompson M, Mallett S, *et al.* Diagnostic accuracy studies: how to report and analyse inconclusive test results. *BMJ* 2013;**346**:f2778. https://doi.org/10.1136/BMJ.F2778.
39. Boxerman JL, Shiroishi MS, Ellingson BM, *et al.* Dynamic susceptibility contrast MR imaging in glioma: review of clinical practice. *Neuroimaging Clin N Am* 2016;**24**(4):649–70. https://doi.org/10.1016/j.mric.2016.06.005.
40. Olivero WC, Dulebohn SC, Lister JR. The use of PET in evaluating patients with primary brain tumours: is it useful? *J Neurol Neurosurg Psychiatry* 1995;**58**(2):250–2. https://doi.org/10.1136/JNNP.58.2.250.
41. Pötzi C, Becherer A, Marosi C, *et al.* [^{11}C] Methionine and [^{18}F] fluorodeoxyglucose PET in the follow-up of glioblastoma multiforme. *J Neurooncol* 2007;**84**(3):305–14. https://doi.org/10.1007/s11060-007-9375-6.
42. Petrovic NS, Grujicic D, Artiko VM, *et al.* Investigation of blood perfusion and metabolic activity of brain tumours in adults by using ^{99m}Tc-methoxyisobutylisonitrile. *Nucl Med Commun* 2010;**31**(11):962–73. https://doi.org/10.1097/MNM.0b013e32833ea6cc.
43. Hakyemez B, Erdogan C, Ercan I, *et al.* High-grade and low-grade gliomas: differentiation by using perfusion MR imaging. *Clin Radiol* 2005;**60**(4):493–502. https://doi.org/10.1016/j.crad.2004.09.009.
44. Alexiou GA, Zikou A, Tsiouris S, *et al.* Correlation of diffusion tensor, dynamic susceptibility contrast MRI and ^{99m}Tc-tetrofosmin brain SPECT with tumour grade and Ki-67 immunohistochemistry in glioma. *Clin Neurol Neurosurg* 2014;**116**:41–5. https://doi.org/10.1016/j.clineuro.2013.11.003.